Label-Free Detection of Doxorubicin in Lake Water by an Electrochemical Aptamer Biosensor

Songjia Luo[1], Lu Wang[1], Hao Qu[1,2,*] and Lei Zheng[1,3]

[1]*School of Food and Biological Engineering, Hefei University of Technology, Hefei 230009, China*

[2]*Engineering Research Center of Bioprocess, Ministry of Education, Hefei University of Technology, Hefei, 230009, China*

[3]*Intelligent Interconnected Systems Laboratory of Anhui Province, Hefei University of Technology, Hefei 230009, China*

Abstract: The application of electrochemical sensors to the detection of real samples is hampered by the fact that the electrode surface is often prone to adsorption of other substances that cause a non-specific current response. In addition, electroactive substances in the actual sample are prone to redox reactions on the electrode surface and affect the detection of target molecules. In this paper, we constructed a novel DOX sensor with excellent selectivity using an aptamer-modified gold electrode and used it for the label-free rapid detection of DOX in lake water. DOX molecules in solution can be captured by the aptamers immobilised on the surface of the gold electrode, followed by the DOX molecules getting electrons on the surface of the electrode and undergoing a reduction reaction. Aptamers give electrochemical sensors excellent sensitivity and selectivity. Finally, the electrochemical aptamer biosensor was successfully applied to detect DOX in lake water with a detection limit of 30 nmol/L and a detection range of 30 nmol/L – 10 μmol/L.

Keywords: Electrochemical aptamer biosensor, Doxorubicin detection, Label-free detection.

1. INTRODUCTION

The extensive use of antibiotics in clinical treatments leads to their introduction into natural environmental waters through human excretion and medical wastewater discharges [1-3]. Doxorubicin (DOX), an anthracycline antibiotic with excellent anticancer activity, has been widely used in the chemotherapy of cancer [4, 5]. Animal studies have shown that DOX is cardiotoxic, embryotoxic and mutagenic [6]. During chemotherapy, DOX may be excreted into the sewage system through the urine of cancer patients [7-9]. Due to incomplete degradation in wastewater treatment systems, DOX enter natural water bodies and groundwater, thus causing serious environmental pollution problems [10]. Therefore, it is of great practical significance to develop a rapid and accurate method for the rapid detection of DOX in environmental waters.

Currently, the accurate detection of DOX is mainly performed using classical analytical methods including chromatography, fluorescence spectroscopy, and UV-Vis spectroscopy [11-13]. However, these methods require large instruments and specialised personnel to operate. Compared with these classical analytical methods, electrochemical sensors have the advantages of low cost, fast response and simple operation, and are suitable for the rapid detection of DOX in environmental waters [14-16]. DOX is susceptible to redox reactions on the electrode surface due to its electrochemically active groups (quinone, hydroxyquinone) [17]. Therefore, researchers have mostly focused on modifying electrodes using nanomaterials to improve the detection sensitivity of the DOX sensors [18-20]. Th. Abhishek Singh *et al*. [21] synthesised a carbon dots/magnesium oxide (CDs/MgO) nanomaterial using hydrothermal method. Modification of SPCE electrode using this nanomaterial significantly enhanced the electrochemically active surface area of the working electrode. DOX was detected using cyclic voltammetry with a detection limit of 0.09 μmol/L. Haiyan Zhao *et al*. [22] developed a sensitive DOX electrochemical sensor based on covalent organic skeleton electrode materials modified with gold nanoparticles and multi-walled carbon nanotubes (AuNPs@COFs-MWCNTs). AuNPs@COFs-MWCNTs significantly enhanced the electrocatalytic performance of the electrodes with a detection limit for DOX as low as 16 nmol/L.

Although the detection of target molecules using electrochemical analytical methods such as square wave voltammetry (SWV) is performed with good selectivity due to the specific redox peaks of the target molecules [23, 24]. However, when electrochemical sensors are applied to the analysis and detection of

---

*Address correspondence to this author at the School of Food and Biological Engineering, Hefei University of Technology, Hefei 230009, China;
E-mail: quhao@hfut.edu.cn

real samples, the electrode surface tends to adsorb macromolecules, resulting in a non-specific current response [25, 26]. Aptamers are oligonucleotide sequences obtained by *in vitro* screening that recognise specific target molecules [27, 28]. Because aptamers have the advantages of low synthetic cost, high specificity and easy modification, electrochemical aptamer biosensors have attracted wide attention in recent years [29-32]. Nicole Bahner *et al*. [33] developed an impedance-based electrochemical biosensor for the detection of DOX using aptamers and 6-Mercapto-1-hexanol (MCH)-modified gold electrodes. This electrochemical biosensor requires measurement of electrochemical impedance spectroscopy (EIS) in [Fe $(CN)_6]^{3+/4+}$ solutions. Therefore, the development of reagent-free electrochemical aptamer sensors for real-time monitoring of DOX is essential.

In this work, we developed a label-free electrochemical aptamer biosensor for the rapid detection of DOX in lake water. The aptamer was self-assembled onto the surface of a gold electrode by Au-S bonding, and then the electrode was closed using MCH. The aptamer modified on the surface of the electrode traps DOX molecules in the detection solution, and when the electrode is tested using square-wave voltammetry, the DOX undergoes a redox reaction on the surface of the electrode, gaining electrons and generating a reduction current. Experimental results showed that the prepared

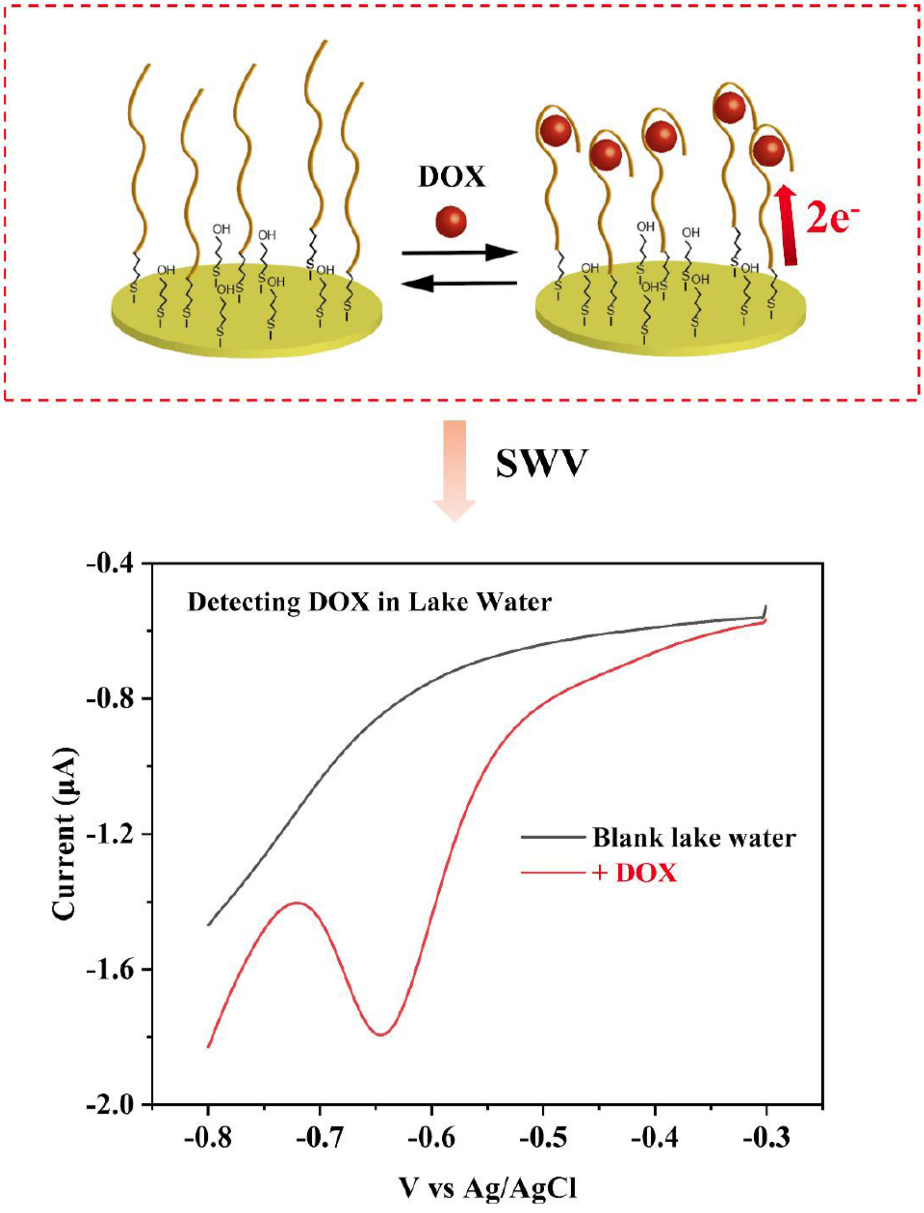

Scheme 1: Schematic diagram of label-free detection of DOX in lake water by electrochemical aptamer sensors.

electrochemical aptamer biosensor could accurately detect DOX in spiked lake water samples in the range of 30 nmol/L - 10 μmol/L, and the sensor had excellent selectivity and detection sensitivity.

2. MATERIALS AND METHODS

2.1. Materials and Reagents

Gold working electrode, Pt wire counter electrode, and Ag/AgCl reference electrode were purchased from CH Instruments, Inc. arsenic nitrate, copper nitrate, mercury nitrate, lead nitrate purchased from Guobiao (Beijing) Testing & Certification Co., Ltd. Tris(2-carboxyethyl) phosphine hydrochloride (TCEP), 6-Mercapto-1-hexanol (MCH), potassium ferricyanide, potassium ferrocyanide trihydrate, potassium chloride (KCl), and sodium hydroxide (NaOH) were obtained from Aladdin Biochemical Technology Co., Ltd. (Shanghai, China). Doxorubicin hydrochloride (DOX), kanamycin sulfate (Kana), and PBS buffer (PH 7.2-7.4) were purchased from Biotech Bioengineering (Shanghai, China) Co., Ltd. Concentrated sulfuric acid (H_2SO_4) was obtained from Sinopharm Chemical Reagent Co., Ltd. (Shanghai, China). Enrofloxacin hydrochloride (ENR), tetracycline hydrochloride (TET), chlorotetracycline hydrochloride (CHT), chloramphenicol (CHP), ciprofloxacin hydrochloride (CIP), and ofloxacin hydrochloride (OFL) were obtained from Macklin Inc. The Lake water sample was taken from Liren Lake of Hefei University of Technology. Water quality parameters (biochemical oxygen demand (BOD): 6.32 mg/L, total dissolved solids (TDS): 159 mg/L, electrical conductivity (EC): 218μS/cm, oxidation-reduction potential (ORP):74 mV, total hardness (TH):69 mg/L, PH:7.15).

The aptamer was synthesized and purified by Biotech Bioengineering Co., Ltd., with the 5' end modified with HS-SH-$(CH_2)_6$, and the sequence of the nucleic acid aptamer [34] was 5 ' - HS- S-$(CH_2)_6$ - ACC ATC TGT GTA AGG GGT AAG GGG TGG T - 3'. The aptamer powder was dissolved using PBS to a concentration of 100 μM and then stored in a -20°C refrigerator.

2.2. Pretreatment and Modification Process of Gold Electrodes

The working electrodes were first polished with 0.05 μm Al_2O_3 powder for 2 minutes, and then the electrodes were cleaned sequentially by ultrasonic cleaning in anhydrous ethanol and deionised water for 5 minutes. The working electrode was then connected to an electrochemical workstation for electrochemical cleaning. (1) 300 cycles were scanned using cyclic voltammetry in 0.5 mol/L NaOH solution with a scanning voltage range of -1 V to -1.6 V and a scanning rate of 1 V/s. (2) 20 cycles were scanned using cyclic voltammetry in 0.1 mol/L H_2SO_4 / 0.01 mol/L KCl solution with a scan voltage range of 0.2 V-1.5 V and a scan rate of 0.1 V/s. Finally, the electrodes were blown dry using nitrogen.

2 μL of aptamer solution (100 mol/L) was taken and mixed well by adding 4 μL of TCEP solution (5 mmol/L) and incubated for 1 hour at room temperature, then the aptamer solution was diluted using PBS solution to make it 500 nmol/L. The working electrode was inserted into the aptamer solution and incubated for 2 hours at room temperature, followed by rinsing the electrode twice with PBS solution. Finally, the working electrode was immersed into the MCH solution (2 mmol/L) and placed in a 4°C refrigerator overnight.

2.3. Electrochemical Testing

EIS was tested in solutions containing 0.1 mol/L KCl and 5 mmol/L $[Fe\ (CN)_6]^{3-/4-}$ (potential: 0.2 V; frequency range: 0.1 Hz - 100 kHz). SWV measurements were performed in PBS solution and lake water with the following parameter settings: scanning voltage range of -0.3 V to -0.8 V, potential step of 0.001 V, amplitude of 0.025 V, scanning frequency of 100 Hz, and sensitivity of 1×10^{-5} A/V.

3. RESULTS AND DISCUSSION

3.1. Electrochemical Impedance Spectroscopy of Modified Electrodes

EIS tests were carried out in $[Fe\ (CN)_6]^{3-/4-}$ solution to characterise the change in surface charge transfer resistance (R_{ct}) of the electrode modification process. As shown in Figure **1**, the diameter of the semicircle in the curve represents the value of the electrode Rct. Where the R_{ct} of the bare gold electrode was about 237 Ω, when the aptamer was modified, the R_{ct} increased to about 1342 Ω. Finally, the R_{ct} further increased to about 3302 Ω when the MCH closed electrode was used. The significant increase in the R_{ct} value of the gold electrode surface indicates that the aptamer was successfully modified to the electrode surface and that MCH successfully closed the remaining active site of the gold electrode.

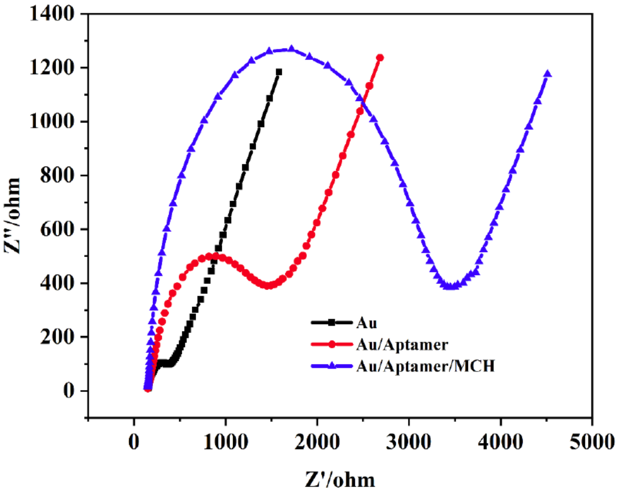

Figure 1: Electrochemical impedance spectroscopy of electrode modification.

3.2. Detection of DOX in PBS

We first tested the detection performance of the sensor in PBS buffer, as shown in Figure **2**, when DOX was not present in the PBS buffer, the SWV curve did not show any obvious reduction peaks around 0.61V. When the concentration of added DOX reached 30 nmol/L, an obvious reduction peak appeared around 0.61 V, which was due to the reduction reaction of DOX molecules on the electrode surface. And with the increase of DOX concentration, the peak current of the reduction peak increased significantly, which was due to the reduction reaction of more DOX molecules on the electrode surface. The aptamer modified on the surface of the electrode traps the DOX molecules in PBS, which undergo a reduction reaction driven by the scanning voltage to obtain electrons, generating a Faraday current. Three consecutive measurements of 1 μM DOX were performed using the prepared sensor and the experimental results are shown in Table **1** with a relative standard deviation of 7.7%. This detection mechanism is similar to the catalytic reaction of an enzyme, so we used the Michaelis-Menten equation to fit the calibration curve. Change in DOX concentration

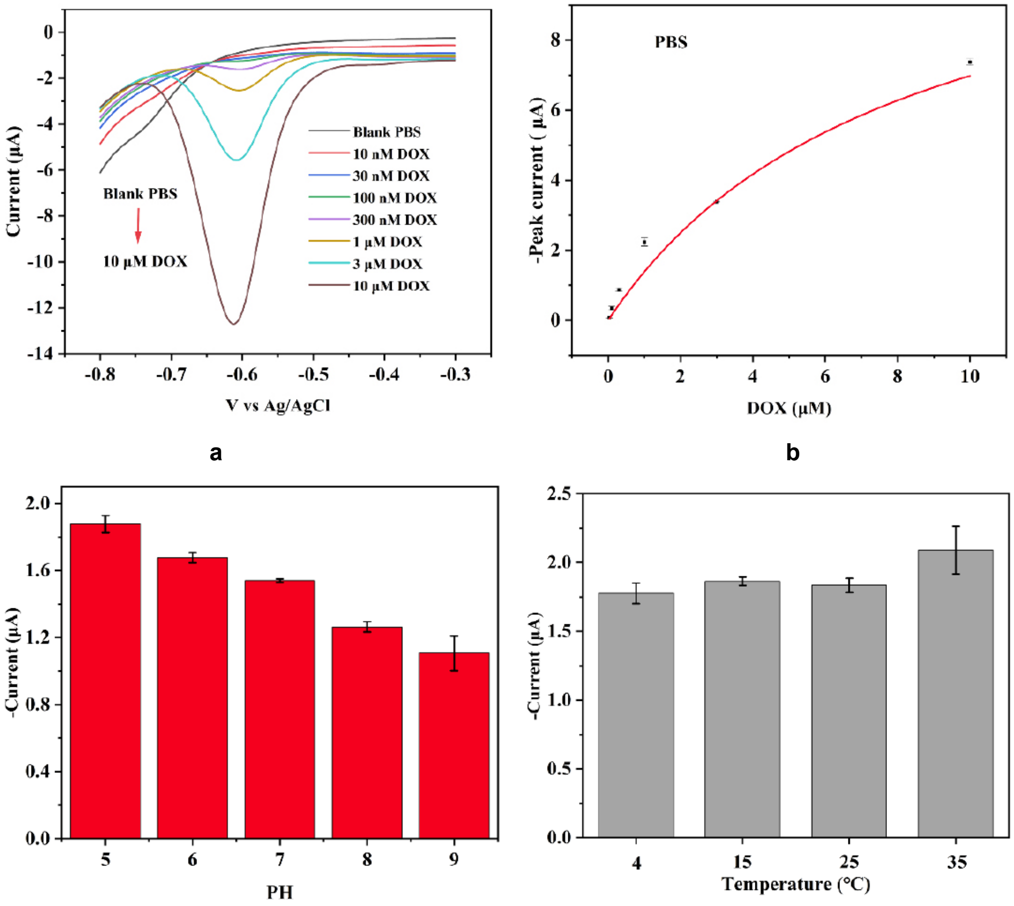

a b

c d

Figure 2: (**a**) SWVs curve of the DOX sensor in PBS, (**b**) calibration curve of the DOX sensor in PBS, (**c**) effect of PH on the detection performance of DOX sensors (1μM DOX), (**d**) effect of temperature on the detection performance of DOX sensors (1μM DOX). The error bars indicate the standard deviation of three consecutive measurements.

Table 1: Reproducibility of DOX (1 μmol/L) by the Biosensor

Test	Test 1	Test 2	Test 3	Average	RSD (%)
Current (μA)	-2.37	-2.51	-2.15	-2.34	7.7

with respect to the peak current is in accordance with the Michaelis-Menten equation [35].

$$PC = PC_{\max}\frac{[DOX]}{K_m + [DOX]} \tag{1}$$

where PC denotes the peak current, PC_{max} represents the maximum value of the peak current, [DOX] is the molar concentration of DOX, and K_m is the dissociation constant.

The calibration curve of the sensor in PBS was obtained by nonlinear fitting of the measured data using OriginPro 2021, where PC_{max}=12.65±3.74 μA, K_m=8.12±3.35 μmol/L, R^2=0.996.

3.3. Selective Testing of DOX Sensor

To test the selectivity of the electrochemical aptamer sensor, we chose several common antibiotics and heavy metals that may be present in lake water. As shown in Figure **3ab**, when these interfering substances were added to the solution, no obvious reduction peaks appeared in the SWV curves, whereas when 1 μmol/L DOX was added to the solution, the reduction peaks of DOX molecules appeared in the SWV curves. In addition, we chose the structural analogues of DOX, tetracycline (TET) and chlortetracycline (CHT), as interfering substances during the selectivity test. As shown in Figure **3a**, the addition of 10 μmol/L of tetracycline and chlortetracycline showed no obvious reduction peaks, which indicates that the sensor has good anti-interference ability. The selectivity experiments showed that the aptamers endowed the electrochemical sensor with excellent selectivity and anti-interference ability.

3.4. Electrochemical Aptamer Biosensor Detects DOX in Lake Water

Finally, we tested the detection performance of the sensor in real lake water samples. The lake water sample was not pre-treated and then the sensor was immersed into the lake water, followed by adding DOX to it and recording the SWV curve after 5 minutes. As shown in Figure **4a**, when 30 nmol/L DOX was added to the lake water sample, the SWV curve showed a reduction peak at -0.6 V, and the peak current of the reduction peak increased significantly with the increase of the concentration of DOX in the lake water sample. As shown in Figure **4b**, the calibration curve for the sensor to detect DOX in real lake water samples was obtained by nonlinear fitting using equation 1, where PC_{max}=336.69±44.83 μA, K_m=4.21±0.71 μmol/L, R^2=0.996. The experimental results show that the prepared DOX sensor has excellent detection performance with a detection limit of 30 nmol/L and a detection range of 30 nmol/L – 10 μmol/L when working in real lake water samples. As shown in Table **2**, which shows the recently reported DOX sensors, we have prepared sensors with low detection limits as well as a wide detection range for practical use.

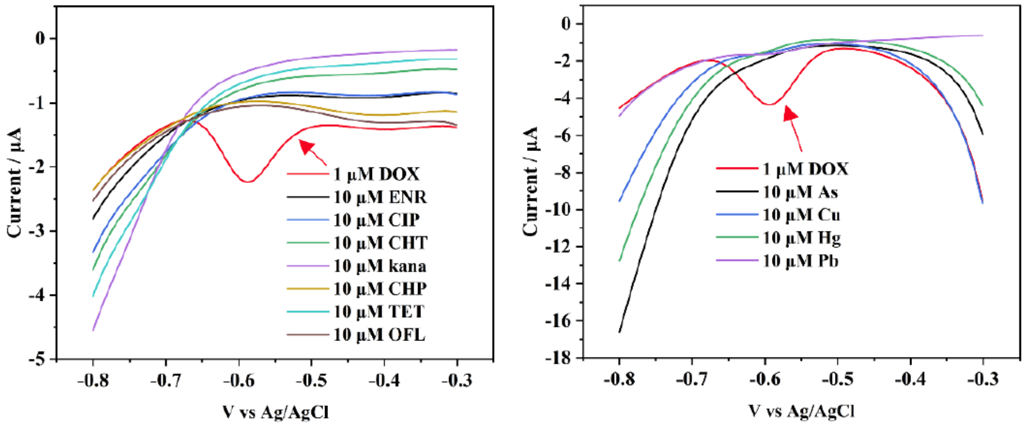

a b

Figure 3: Selectivity test of DOX sensor. (**a**) SWV curves after addition of other antibiotics (10 μmol/L) and DOX (1 μmol/L) to the solution, (**b**) SWV curves after addition of heavy metal ions (10 μmol/L) and DOX (1 μmol/L) to the solution.

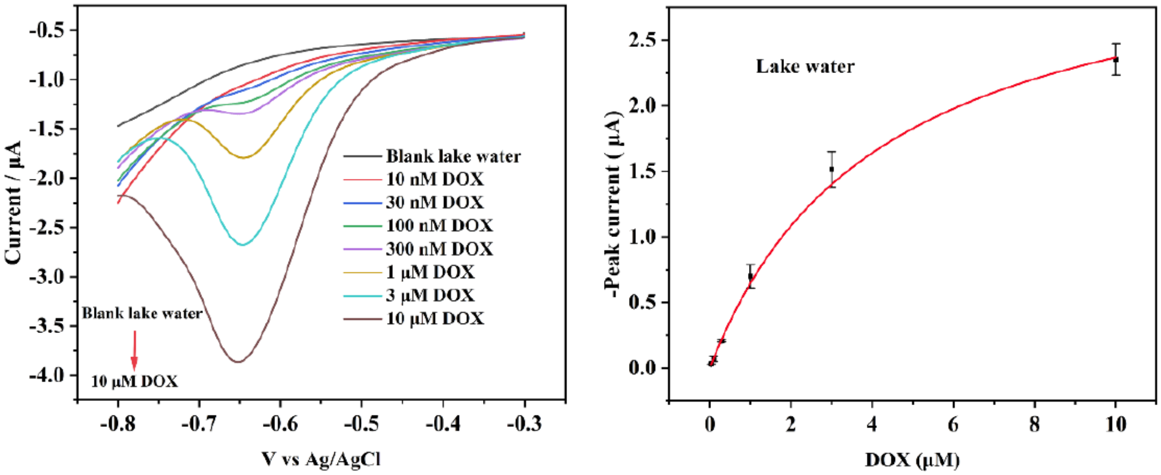

a **b**

Figure 4: Electrochemical aptamer biosensor detects DOX in lake water. (**a**) SWV curves of lake water samples after addition of different concentrations of DOX, (**b**) calibration curve of the sensor for DOX detection in lake water samples.

Table 2: Comparison of Analytical Performance for DOX between this Work and other Representative Publications

Method	Material	LOD (µM)	Detection range (µM)	Real Sample	Reference
EIS	Aptamer/MCH/Au	0.028	0.031–0.125	water	33
Fluorescence	Apt-NaYF$_4$:Yb/Er/Nd@NaYF$_4$:Nd	0.5	0.5 ‒ 55	human urine	36
FRET	MUA-CDs	0.66	0.25 ‒ 19.96	mice serum, human urine	37
Fluorescence	Bimetallic Au/Ag nanoclusters	0.003	2.5 ‒ 150	human serum	38
DPV	MB@MWCNTs/UiO-66-NH$_2$	0.051	0.1–75	human saliva	39
SWV	rGO/AuNPs/Aptamer	0.1	0.3–6	human serum	40
SWV	Aptamer/MCH/Au	0.03	0.03–10	Lake water	This work

4. CONCLUSION

In this paper, we prepared an electrochemical aptamer biosensor with high selectivity for the rapid detection of DOX in lake water. The aptamer immobilised on the surface of the electrode specifically recognises DOX molecule, which undergo a reduction reaction on the surface of the gold electrode to generate a reduction current. The excellent sensitivity and selectivity of the sensor after modifying the gold electrode with the aptamer and MCH was attributed to the fact that the aptamer could enrich DOX molecules on the electrode surface. The actual sample detection experiments showed that the detection limit of the sensor for DOX in lake water was 30 nmol/L, and the detection range was 30 nmol/L ‒ 10 µmol/L. This work provides a new idea for the construction of electrochemical biosensors with high selectivity.

ACKNOWLEDGEMENT

This work was supported by the Sub-theme of National Key Research and Development Program (2022YFB3207204), the National Natural Science Foundation of China (32172294, 31901406), and the Key Science & Technology Specific Projects of Anhui Province (2020b06050001).

REFERENCES

[1] Liu C, Li B, Liu M, Mao S. Demand, status, and prospect of antibiotics detection in the environment. Sensors and Actuators B: Chemical 2022; 369: 132383. https://doi.org/10.1016/j.snb.2022.132383

[2] Wang Q, Zhao W-M. Optical methods of antibiotic residues detections: A comprehensive review. Sensors and Actuators B: Chemical 2018; 269: 238-256. https://doi.org/10.1016/j.snb.2018.04.097

[3] Zhou Y-J, Zhu F, Zheng D-Y, Gao M-M, Guo B-F, Zhang N, Meng Y, Wu G-l, Zhou Y-l, Huo X. Detection of antibiotics in

the urine of children and pregnant women in Jiangsu, China. Environmental Research 2021; 196: 110945.
https://doi.org/10.1016/j.envres.2021.110945

[4] Mescheryakova SA, Matlakhov IS, Strokin PD, Drozd DD, Goryacheva IY, Goryacheva OA. Fluorescent Alloyed CdZnSeS/ZnS Nanosensor for Doxorubicin Detection Biosensors 2023; 13: 596.
https://doi.org/10.3390/bios13060596

[5] Zhu J, Chu H, Shen J, Wang C, Wei Y. Green preparation of carbon dots from plum as a ratiometric fluorescent probe for detection of doxorubicin. Optical Materials 2021; 114: 110941.
https://doi.org/10.1016/j.optmat.2021.110941

[6] Amy DH, Alex L, Steffi T, Angela FD, Nicole AB. Adverse Effects of Doxorubicin and Its Metabolic Product on Cardiac RyR2 and SERCA2A. Molecular Pharmacology 2014; 86(4): 438.
https://doi.org/10.1124/mol.114.093849

[7] Lv N, Qiu X, Han Q, Xi F, Wang Y, Chen J. Anti-Biofouling Electrochemical Sensor Based on the Binary Nanocomposite of Silica Nanochannel Array and Graphene for Doxorubicin Detection in Human Serum and Urine Samples Molecules 2022; 27: 8640.
https://doi.org/10.3390/molecules27248640

[8] Laura Soriano M, Carrillo-Carrion C, Ruiz-Palomero C, Valcárcel M. Cyclodextrin-modified nanodiamond for the sensitive fluorometric determination of doxorubicin in urine based on its differential affinity towards β/γ-cyclodextrins. Microchimica Acta 2018; 185(2): 115.
https://doi.org/10.1007/s00604-017-2660-y

[9] Sottani C, Rinaldi P, Leoni E, Poggi G, Teragni C, Delmonte A, Minoia C. Simultaneous determination of cyclophosphamide, ifosfamide, doxorubicin, epirubicin and daunorubicin in human urine using high-performance liquid chromatography/electrospray ionization tandem mass spectrometry: bioanalytical method validation. Rapid Communications in Mass Spectrometry 2008; 22(17): 2645-2659.
https://doi.org/10.1002/rcm.3657

[10] Mahnik SN, Lenz K, Weissenbacher N, Mader RM, Fuerhacker M. Fate of 5-fluorouracil, doxorubicin, epirubicin, and daunorubicin in hospital wastewater and their elimination by activated sludge and treatment in a membrane-bio-reactor system. Chemosphere 2007; 66(1): 30-37.
https://doi.org/10.1016/j.chemosphere.2006.05.051

[11] Aboras SI, Korany MA, Abdine HH, Ragab MA A, El Diwany A, Agwa MM. HPLC with fluorescence detection for the bioanalysis and pharmacokinetic study of Doxorubicin and Prodigiosin loaded on eco-friendly casein nanomicelles in rat plasma. Journal of Chromatography B 2021; 1187: 123043.
https://doi.org/10.1016/j.jchromb.2021.123043

[12] Sikora T, Morawska K, Lisowski W, Rytel P, Dylong A. Application of Optical Methods for Determination of Concentration of Doxorubicin in Blood and Plasma Pharmaceuticals 2022; 15: 112.
https://doi.org/10.3390/ph15020112

[13] Mohammadinejad A, Abnous K, Alinezhad Nameghi M, Yahyazadeh R, Hamrah S, Senobari F, Mohajeri SA. Application of green-synthesized carbon dots for imaging of cancerous cell lines and detection of anthraquinone drugs using silica-coated CdTe quantum dots-based ratiometric fluorescence sensor. Spectrochimica Acta Part A: Molecular and Biomolecular Spectroscopy 2023; 288: 122200.
https://doi.org/10.1016/j.saa.2022.122200

[14] Florea A, Guo Z, Cristea C, Bessueille F, Vocanson F, Goutaland F, Dzyadevych S, Săndulescu R, Jaffrezic-Renault N. Anticancer drug detection using a highly sensitive molecularly imprinted electrochemical sensor based on an electropolymerized microporous metal organic framework. Talanta 2015; 138: 71-76.
https://doi.org/10.1016/j.talanta.2015.01.013

[15] Lima HRS, da Silva JS, de Oliveira Farias EA, Teixeira PRS, Eiras C, Nunes L, César C. Electrochemical sensors and biosensors for the analysis of antineoplastic drugs. Biosensors and Bioelectronics 2018; 108: 27-37.
https://doi.org/10.1016/j.bios.2018.02.034

[16] Hashemi SA, Mousavi SM, Bahrani S, Gholami A, Chiang W-H, Yousefi K, Omidifar N, Rao NV, Ramakrishna S, Babapoor A, Lai CW. Bio-enhanced polyrhodanine/graphene Oxide/Fe3O4 nanocomposite with kombucha solvent supernatant as ultra-sensitive biosensor for detection of doxorubicin hydrochloride in biological fluids. Materials Chemistry and Physics 2022; 279: 125743.
https://doi.org/10.1016/j.matchemphys.2022.125743

[17] Abbasi M, Ezazi M, Jouyban A, Lulek E, Asadpour-Zeynali K, Ertas YN, Houshyar J, Mokhtarzadeh A, Soleymani J. An ultrasensitive and preprocessing-free electrochemical platform for the detection of doxorubicin based on tryptophan/polyethylene glycol-cobalt ferrite nanoparticles modified electrodes. Microchemical Journal 2022; 183: 108055.
https://doi.org/10.1016/j.microc.2022.108055

[18] Guo H, Jin H, Gui R, Wang Z, Xia J, Zhang F. Electrodeposition one-step preparation of silver nanoparticles/carbon dots/reduced graphene oxide ternary dendritic nanocomposites for sensitive detection of doxorubicin. Sensors and Actuators B: Chemical 2017; 253: 50-57.
https://doi.org/10.1016/j.snb.2017.06.095

[19] Kalambate PK, Li Y, Shen Y, Huang Y. Mesoporous Pd@Pt core–shell nanoparticles supported on multi-walled carbon nanotubes as a sensing platform: application in simultaneous electrochemical detection of anticancer drugs doxorubicin and dasatinib. Analytical Methods 2019; 11(4): 443-453.
https://doi.org/10.1039/C8AY02381F

[20] Kondori T, Tajik S, Akbarzadeh TN, Beitollahi H, Graiff C. Screen-printed electrode modified with Co-NPs, as an electrochemical sensor for simultaneous determination of doxorubicin and dasatinib. Journal of the Iranian Chemical Society 2022; 19(11): 4423-4434.
https://doi.org/10.1007/s13738-022-02613-9

[21] Abhishek Singh T, Sharma V, Thakur N, Tejwan N, Sharma A, Das J. Selective and sensitive electrochemical detection of doxorubicin via a novel magnesium oxide/carbon dot nanocomposite based sensor. Inorganic Chemistry Communications 2023; 150: 110527.
https://doi.org/10.1016/j.inoche.2023.110527

[22] Zhao H, Shi K, Zhang C, Ren J, Cui M, Li N, Ji X, Wang R. Spherical COFs decorated with gold nanoparticles and multiwalled carbon nanotubes as signal amplifier for sensitive electrochemical detection of doxorubicin. Microchemical Journal 2022; 182: 107865.
https://doi.org/10.1016/j.microc.2022.107865

[23] Sebokolodi TI, Sipuka DS, Tsekeli TR, Nkosi D, Arotiba OA. An electrochemical sensor for caffeine at a carbon nanofiber modified glassy carbon electrode. Journal of Food Measurement and Characterization 2022; 16(4): 2536-2544.
https://doi.org/10.1007/s11694-022-01365-7

[24] Cho CH, Kim JH, Kim J, Yun JW, Park TJ, Park JP. Re-engineering of peptides with high binding affinity to develop an advanced electrochemical sensor for colon cancer diagnosis. Analytica Chimica Acta 2021; 1146: 131-139.
https://doi.org/10.1016/j.aca.2020.11.011

[25] Ma K, Yang L, Liu J, Liu J. Electrochemical Sensor Nanoarchitectonics for Sensitive Detection of Uric Acid in Human Whole Blood Based on Screen-Printed Carbon Electrode Equipped with Vertically-Ordered Mesoporous Silica-Nanochannel Film Nanomaterials 2022; 12(7): 1157.
https://doi.org/10.3390/nano12071157

[26] Huang L, Su R, Xi F. Sensitive detection of noradrenaline in human whole blood based on Au nanoparticles embedded

vertically-ordered silica nanochannels modified pre-activated glassy carbon electrodes. Frontiers in Chemistry 2023; 11. https://doi.org/10.3389/fchem.2023.1126213

[27] Qu H, Ma Q, Wang L, Mao Y, Eisenstein M, Soh HT, Zheng L. Measuring Aptamer Folding Energy Using a Molecular Clamp. Journal of the American Chemical Society 2020; 142(27): 11743-11749. https://doi.org/10.1021/jacs.0c01570

[28] Qu H, Csordas AT, Wang J, Oh SS, Eisenstein MS, Soh HT. Rapid and Label-Free Strategy to Isolate Aptamers for Metal Ions. ACS Nano 2016; 10(8): 7558-7565. https://doi.org/10.1021/acsnano.6b02558

[29] Wang R, Cao Y, Qu H, Wang Y, Zheng L. Label-free detection of Cu(II) in fish using a graphene field-effect transistor gated by structure-switching aptamer probes. Talanta 2022; 237: 122965. https://doi.org/10.1016/j.talanta.2021.122965

[30] Wang Y, Bi Y, Wang R, Wang L, Qu H, Zheng L. DNA-Gated Graphene Field-Effect Transistors for Specific Detection of Arsenic(III) in Rice. Journal of Agricultural and Food Chemistry 2021; 69(4): 1398-1404. https://doi.org/10.1021/acs.jafc.0c07052

[31] Leung KK, Downs AM, Ortega G, Kurnik M, Plaxco KW. Elucidating the Mechanisms Underlying the Signal Drift of Electrochemical Aptamer-Based Sensors in Whole Blood. ACS Sensors 2021; 6(9): 3340-3347. https://doi.org/10.1021/acssensors.1c01183

[32] Idili A, Parolo C, Alvarez-Diduk R, Merkoçi A. Rapid and Efficient Detection of the SARS-CoV-2 Spike Protein Using an Electrochemical Aptamer-Based Sensor. ACS Sensors 2021; 6(8): 3093-3101. https://doi.org/10.1021/acssensors.1c01222

[33] Bahner N, Reich P, Frense D, Menger M, Schieke K, Beckmann D. An aptamer-based biosensor for detection of doxorubicin by electrochemical impedance spectroscopy. Analytical and Bioanalytical Chemistry 2018; 410(5): 1453-1462. https://doi.org/10.1007/s00216-017-0786-8

[34] Ferguson BS, Hoggarth DA, Maliniak D, Ploense K, White RJ, Woodward N, Hsieh K, Bonham AJ, Eisenstein M, Kippin TE, Plaxco KW, Soh HT. Real-Time, Aptamer-Based Tracking of Circulating Therapeutic Agents in Living Animals. Science Translational Medicine 2013; 5(213): 213ra165. https://doi.org/10.1126/scitranslmed.3007095

[35] Biaglow A, Erickson K, McMurran S. Enzyme Kinetics and the Michaelis-Menten Equation. PRIMUS 2010; 20(2): 148-168. https://doi.org/10.1080/10511970903486491

[36] Mo J, Wang S, Zeng J, Ding X. Aptamer-based Upconversion Fluorescence Sensor for Doxorubicin Detection. Journal of Fluorescence 2023; 33(5): 1897-1905. https://doi.org/10.1007/s10895-023-03184-5

[37] Zhang L, Xing H, Liu W, Wang Z, Hao Y, Wang H, Dong W, Liu Y, Shuang S, Dong C, Gong X. 11-Mercaptoundecanoic Acid-Functionalized Carbon Dots As a Ratiometric Optical Probe for Doxorubicin Detection. ACS Applied Nano Materials 2021; 4(12): 13734-13746. https://doi.org/10.1021/acsanm.1c03141

[38] Meng F, Gan F, Ye G. Bimetallic gold/silver nanoclusters as a fluorescent probe for detection of methotrexate and doxorubicin in serum. Microchimica Acta 2019; 186(6): 371. https://doi.org/10.1007/s00604-019-3477-7

[39] Rong S, Zou L, Meng L, Yang X, Dai J, Wu M, Qiu R, Tian Y, Feng X, Ren X, Jia L, Jiang L, Hang Y, Ma H, Pan H. Dual function metal-organic frameworks based ratiometric electrochemical sensor for detection of doxorubicin. Analytica Chimica Acta 2022; 1196: 339545. https://doi.org/10.1016/j.aca.2022.339545

[40] Kong F, Luo J, Jing L, Wang Y, Shen H, Yu R, Sun S, Xing Y, Ming T, Liu M, Jin H, Cai X. Reduced Graphene Oxide and Gold Nanoparticles-Modified Electrochemical Aptasensor for Highly Sensitive Detection of Doxorubicin. Nanomaterials 2023; 13: 1223. https://doi.org/10.3390/nano13071223

Received on 08-10-2023 Accepted on 26-10-2023 Published on 24-11-2023

https://doi.org/10.12970/2311-1755.2023.11.01